J|A|C|S
COMMUNICATIONS

Published on Web 05/27/2007

Long-Range Structural Restraints in Spin-Labeled Proteins Probed by Solid-State Nuclear Magnetic Resonance Spectroscopy

Philippe S. Nadaud, Jonathan J. Helmus, Nicole Höfer,† and Christopher P. Jaroniec*

Department of Chemistry, The Ohio State University, Columbus, Ohio 43210

Received April 3, 2007; E-mail: jaroniec@chemistry.ohio-state.edu

Magic-angle spinning (MAS) solid-state nuclear magnetic resonance (SSNMR) spectroscopy is rapidly developing as a technique for the atomic-level characterization of structure and dynamics of biomacromolecules not amenable to analysis by X-ray crystallography or solution NMR.[1−5] While nearly complete resonance assignments have been achieved for multiple ^{13}C,^{15}N-enriched proteins up to ∼100 aa,[1,2] enabling the determination of relatively high-resolution 3D protein structures in several cases,[6−8] studies of this type are generally hampered by the availability of a limited number of long range (>5 Å) structural restraints.

Here we investigate the possibility of deriving long range (∼10 to 20 Å) restraints from MAS SSNMR spectra of ^{13}C,^{15}N-enriched proteins containing a covalently attached paramagnetic moiety. In general, the presence of unpaired electrons leads to electron-nucleus distance-dependent NMR chemical shift changes and enhanced longitudinal and transverse relaxation rates,[9,10] and these effects have been successfully exploited in solution-state NMR studies of macromolecular structure.[11,12] On the other hand, the majority of MAS NMR studies of paramagnetic solids to date have been carried out on metal coordination complexes,[13−17] and only very recently have the initial applications to paramagnetic metalloproteins been reported.[18−20] We focus here on proteins containing a bound nitroxide spin label. Nitroxide radicals, characterized by relatively large electronic relaxation time constants (T_{1e}, $T_{2e} \geq \sim 100$ ns) and small *g*-anisotropy,[10,11,21] are expected to significantly enhance the transverse relaxation of the neighboring nuclei in immobilized proteins (with rate constant $R_2 \propto \gamma_I^2/r^6$, where γ_I is the gyromagnetic ratio of the nuclear spin *I* and *r* is the electron-nucleus distance), while generating negligible pseudocontact shifts.[10] A nitroxide side-chain (R1) (or its diamagnetic analogue, R1′, used here as a negative control) can be incorporated into proteins using the site-directed spin-labeling approach developed by Hubbell and co-workers[22] (Figure S1, Supporting Information), where a cysteine residue is introduced at the desired position in the protein using site-directed mutagenesis followed by the specific reaction of the thiol group with a suitable reagent.

A model 56 aa protein, B1 immunoglobulin-binding domain of protein G (GB1), was used in this study. GB1, which contains no native cysteines, has been extensively studied using biophysical and spectroscopic techniques, and detailed information about its structure, dynamics, and folding is available, including 3D solution[23] and crystal[24] structures and the complete ^{13}C and ^{15}N resonance assignments in the solid state.[25] R1 and R1′ side-chains were incorporated at solvent-exposed sites in the α-helix (residue 28) and β4-strand (residue 53) as described in the Supporting Information (for brevity the proteins are named 28R1, 28R1′, 53R1, and 53R1′). Solution and SSNMR chemical shifts, and solution transverse relaxation enhancements reveal that these GB1 analogues retain the wild-type fold (Figures S2−S5). SSNMR measurements were performed on (i) microcrystalline ^{13}C,^{15}N-labeled diamagnetic proteins (28R1′ and 53R1′) and (ii) ^{13}C,^{15}N-28R1 (53R1) diluted in a diamagnetic matrix by cocrystallization with natural abundance 28R1′ (53R1′) in ∼1:3 molar ratio (to minimize intermolecular electron−nuclear dipolar couplings).

2D ^{15}N-$^{13}C^{\alpha}$ spectra of 53R1/53R1′ and 28R1/28R1′ acquired at ∼11 kHz MAS rate are shown in Figure 1A,D. Backbone ^{15}N and ^{13}C assignments for 28R1′ and 53R1′ (Figure S5) were obtained using 2D ^{15}N-($^{13}C^{\alpha}$)-^{13}CX, ^{15}N-($^{13}C'$)-^{13}CX, and ^{13}C-^{13}C experiments, and relatively well-resolved correlations (∼50% of residues) are indicated. Notably, ∼25 to 50% of cross-peaks exhibit significantly reduced intensities in the R1 spectra relative to R1′. In addition, ^{15}N-$^{13}C^{\alpha}$ correlations, which are detected in both spectra, display only minor linebroadening for R1 (∼5 to 30 Hz for ^{13}C and ∼2 to 10 Hz for ^{15}N), and essentially identical resonance frequencies indicating negligible pseudocontact shifts. Given that 53R1′ and 28R1′ adopt the GB1 fold, the reduced cross-peak intensities in R1 spectra are found to be highly correlated with the proximity of the corresponding nuclei to the spin label. For example, T25 and V29 (α-helix) are among the least affected correlations in the 53R1 spectrum, whereas I6 (β1-strand) and T49 (loop between β3 and β4) peaks are effectively suppressed. While the precise conformation of R1 (and hence the spin-label location) in 53R1 is currently unknown, the $^{1}H^{N}$, ^{15}N, and $^{13}C^{\alpha}$ atoms are likely to be within ∼10 Å of the electron for I6 and T49, and ∼20 Å away for T25 and V29 (Figure S7). This spin topology is roughly reversed in 28R1 (T25/V29 and I6/T49 are ∼5 to 10 Å and ∼15 to 20 Å from the radical, respectively), resulting in T25/V29 (I6/T49) correlations being among those most (least) suppressed. The modulation of peak intensities, based on each residue's proximity to the electron spin (Figure S7), persists throughout both 53R1 and 28R1. Figure 1 shows the relative cross-peak intensities (heights) in R1/R1′ spectra as a function of residue location in the primary (B,E) and tertiary (C,F) protein structure. For 53R1, the relaxation effects due to the spin label are largest for residues in the β1-β4 strands and connecting loops, while for 28R1 the most strongly affected residues are found in the α-helix and adjacent loops. Note that these data are in qualitative agreement with the solution-state paramagnetic relaxation enhancements for 28R1 and 53R1 shown in Figure S4.

Dipolar contributions to ^{1}H, ^{13}C, and ^{15}N transverse relaxation rates due to the spin label were estimated using the Solomon−Bloembergen equation,[9,10] assuming an electron correlation time of 100 ns (Figures S8 and S9). These calculations indicate that the reduced cross-peak intensities in R1 spectra result primarily from the decay of transverse ^{1}H and ^{13}C coherences during ^{1}H-^{15}N and ^{15}N-$^{13}C^{\alpha}$ cross-polarization (CP) steps, respectively, and are further supported by measurements of magnetization decay during spin-lock pulses (Figure S10). Under our experimental conditions (0.15 ms ^{1}H-^{15}N CP, 3 ms ^{15}N-$^{13}C^{\alpha}$ CP), cross-peaks arising from nuclei within ∼10 Å of the spin label are expected to be at most ∼20% as intense for R1 relative to R1′, even in the absence of additional

† On leave from the Department of Chemical and Environmental Sciences, University of Limerick, Limerick, Ireland.

10.1021/ja072349t CCC: $37.00

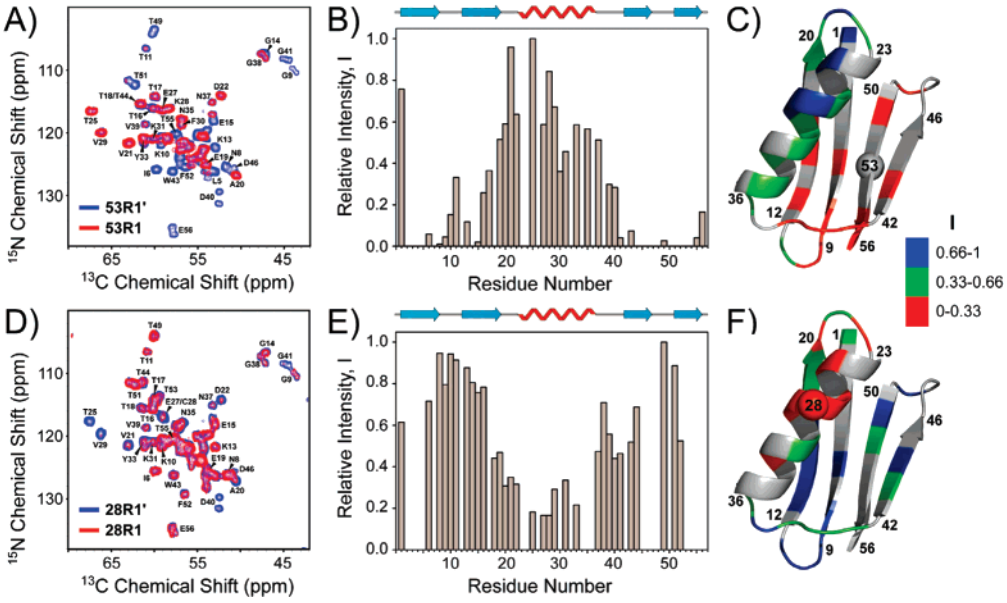

Figure 1. (A) 500 MHz ^{15}N-^{13}C$^{\alpha}$ spectra of 53R1 (red) and 53R1′ (blue) acquired at 11.111 kHz MAS (see Figure S6 for full caption). (B) Relative cross-peak intensities (heights), *I*, in 53R1 and 53R1′ as a function of residue number. To account for possible differences in the amount of ^{13}C,^{15}N-protein in R1 and R1′ samples, we define $I = (I_{R1}/I_{R1'})/(I_{R1}/I_{R1'})_{max}$, where I_{R1} and $I_{R1'}$ are the peak heights in R1 and R1′ spectra and $(I_{R1}/I_{R1'})_{max}$ is the maximum $(I_{R1}/I_{R1'})$ value for the R1/R1′ pair (found here to be ∼0.7 to 0.8). For peaks where no quantitative measurement could be made because of overlap, *I* was set to zero. (C) Ribbon diagram of GB1 (PDB ID: 1pga),[24] with the *I* values mapped onto the structure and color coded as indicated in the figure. Residues for which *I* was not determined are colored in gray, and the R1/R1′ incorporation site is indicated by a sphere on the C$^{\alpha}$ atom. (D−F) Same as panels A−C but for 28R1/28R1′. Typical protein backbone-spin-label distances for secondary structure elements: (28R1) 15−20 Å (β1), 20 Å (β2), 5−10 Å (α), 10−15 Å (β3,β4); (53R1) 10−20 Å (β1), 10−15 Å (β2), 20 Å (α), 10 Å (β3,β4). Estimated uncertainties for individual distances due to unknown R1 conformation are ca. ±2.5 Å (Figure S7).

^{15}N and ^{13}C paramagnetic linebroadening during t_1 and t_2. By contrast, correlations involving nuclei ∼15 to 20 Å away from the radical are expected to retain ∼85 to 95% of the reference intensity and experience only moderate linebroadening in the ^{15}N and ^{13}C dimensions (Figure S8). Although still rather qualitative at this stage, these estimates are consistent with the cross-peak intensities observed experimentally for 28R1/53R1.

In conclusion, we have shown that high-resolution 2D MAS SSNMR spectra recorded on spin-labeled proteins can be used to obtain site-specific structural restraints for nuclei ∼10 to 20 Å from the radical. While the determination of quantitative distance restraints using this approach will, at the very least, require accurate, site-resolved measurements of nuclear relaxation rates (using 3D or 4D pulse schemes incorporating variable relaxation delays), and possibly additional data about electron correlation times and R1 conformation, these restraints provide valuable information about the protein fold on length scales inaccessible to traditional SSNMR methods, even in their current qualitative form. Furthermore, this approach can potentially be extended to editing of SSNMR spectra of larger proteins, with the spin labels used to selectively suppress NMR signals originating from nuclei within ∼10 to 15 Å of the electron and incorporation into proteins of paramagnetic tags with different electronic properties.[26]

Acknowledgment. This research was supported by the Ohio State University. We thank Dr. Angela Gronenborn for the GB1 plasmid, and Drs. Ad Bax, Gareth Eaton, Angela Gronenborn, Junji Iwahara, and Robert Tycko for stimulating discussions.

Supporting Information Available: Experimental part, Figures S1−S10. This material is available free of charge via the Internet at http://pubs.acs.org.

References

(1) McDermott, A. E. *Curr. Opin. Struct. Biol.* **2004**, *14*, 554−561.
(2) Bockmann, A. *C. R. Chim.* **2006**, *9*, 381−392.
(3) Petkova, A. T.; Leapman, R. D.; Guo, Z. H.; Yau, W. M.; Mattson, M. P.; Tycko, R. *Science* **2005**, *307*, 262−265.
(4) Ritter, C.; Maddelein, M. L.; Siemer, A. B.; Luhrs, T.; Ernst, M.; Meier, B. H.; Saupe, S. J.; Riek, R. *Nature* **2005**, *435*, 844−848.
(5) Lange, A.; Giller, K.; Hornig, S.; Martin-Eauclaire, M. F.; Pongs, O.; Becker, S.; Baldus, M. *Nature* **2006**, *440*, 959−962.
(6) Castellani, F.; van Rossum, B.; Diehl, A.; Schubert, M.; Rehbein, K.; Oschkinat, H. *Nature* **2002**, *420*, 98−102.
(7) Zech, S. G.; Wand, A. J.; McDermott, A. E. *J. Am. Chem. Soc.* **2005**, *127*, 8618−8626.
(8) Lange, A.; Becker, S.; Seidel, K.; Giller, K.; Pongs, O.; Baldus, M. *Angew. Chem., Int. Ed.* **2005**, *44*, 2089−2092.
(9) Solomon, I. *Phys. Rev.* **1955**, *99*, 559−565.
(10) Bertini, I.; Luchinat, C. *Coord. Chem. Rev.* **1996**, *150*, 1−292.
(11) Kosen, P. A. *Methods Enzymol.* **1989**, *177*, 86−121.
(12) Bertini, I.; Luchinat, C.; Parigi, G.; Pierattelli, R. *Chembiochem* **2005**, *6*, 1536−49.
(13) Chacko, V. P.; Ganapathy, S.; Bryant, R. G. *J. Am. Chem. Soc.* **1983**, *105*, 5491−5492.
(14) Brough, A. R.; Grey, C. P.; Dobson, C. M. *J. Am. Chem. Soc.* **1993**, *115*, 7318−7327.
(15) Liu, K.; Ryan, D.; Nakanishi, K.; McDermott, A. E. *J. Am. Chem. Soc.* **1995**, *117*, 6897−6906.
(16) Wickramasinghe, N. P.; Ishii, Y. *J. Magn. Reson.* **2006**, *181*, 233−243.
(17) Kervern, G.; Pintacuda, G.; Zhang, Y.; Oldfield, E.; Roukoss, C.; Kuntz, E.; Herdtweck, E.; Basset, J. M.; Cadars, S.; Lesage, A.; Coperet, C.; Emsley, L. *J. Am. Chem. Soc.* **2006**, *128*, 13545−13552.
(18) Jovanovic, T.; McDermott, A. E. *J. Am. Chem. Soc.* **2005**, *127*, 13816−13821.
(19) Pintacuda, G.; Giraud, N.; Pierattelli, R.; Bockmann, A.; Bertini, I.; Emsley, L. *Angew. Chem., Int. Ed.* **2007**, *119*, 1097−1100.
(20) Balayssac, S.; Bertini, I.; Lelli, M.; Luchinat, C.; Maletta, M. *J. Am. Chem. Soc.* **2007**, *129*, 2218−2219.
(21) Eaton, S. S.; Eaton, G. R. In *Distance Measurements in Biological Systems by EPR;* Biological Magnetic Resonance, Vol. 19; Kluwer Academic: New York, 2000.
(22) Hubbell, W. L.; Altenbach, C. *Curr. Opin. Struct. Biol.* **1994**, *4*, 566−573.
(23) Gronenborn, A. M.; Filpula, D. R.; Essig, N. Z.; Achari, A.; Whitlow, M.; Wingfield, P. T.; Clore, G. M. *Science* **1991**, *253*, 657−661.
(24) Gallagher, T.; Alexander, P.; Bryan, P.; Gilliland, G. L. *Biochemistry* **1994**, *33*, 4721−4729.
(25) Franks, W. T.; Zhou, D. H.; Wylie, B. J.; Money, B. G.; Graesser, D. T.; Frericks, H. L.; Sahota, G.; Rienstra, C. M. *J. Am. Chem. Soc.* **2005**, *127*, 12291−12305.
(26) Rodriguez-Castaneda, F.; Haberz, P.; Leonov, A.; Griesinger, C. *Magn. Reson. Chem.* **2006**, *44*, S10−S16.

JA072349T